Supplementary Information

{$Cu_2SiW_{12}O_{40}$}@HKUST-1 synthesized by the one-step solution method with efficient bifunctional activity for supercapacitor and oxygen evolution reaction

Huan Liu[a], Li-Ge Gong[a,b*], Chun-Xiao Wang[a], Chun-Mei Wang[a], Kai Yu[a,b*], Bai-Bin Zhou[a,b*]

POMOFs constructed of polyoxometalates (POMs) and metal-organic frameworks (MOF) are very desirable for high-efficiency supercapacitor performance and electrocatalytic water oxygen evolution reaction, but it is still challenging. Herein, successfully synthesized the {$Cu_2SiW_{12}O_{40}$}@HKUST-1 material through a one-step solution method. The synergy between {$Cu_2SiW_{12}O_{40}$} and HKUST-1 can promote mass/charge transfer and the adsorption/desorption of intermediates on {$Cu_2SiW_{12}O_{40}$}@HKUST-1. In the three-electrode system, {$Cu_2SiW_{12}O_{40}$}@HKUST-1 electrode material has a specific capacitance of 5096.5F g^{-1} when the current density is 1A g^{-1}, after 6000 cycles, the retention rate is 92%, which is much higher than reported in the literature. The symmetrical electrode is assembled with foamed nickel as the current collector, in the 1.0V voltage window, the power density is 510.81W kg^{-1}, and the energy density is 15.31Wh kg^{-1}. In 1.0 M KOH aqueous solution, when the scanning speed is 5mV s^{-1}, the overpotential of electrocatalytic water oxygen evolution reaction(OER) is 340mV (without iR compensation). Especially at high current density, {$Cu_2SiW_{12}O_{40}$}@HKUST-1 shows better performance than commercial RuO_2. Further, it has excellent catalytic durability. It provides a basis for the further application of POMOFs.

Table of Contents

1. Experimental Procedures

1.1 Material characterization method

In the Bruker Ver Tex 80 Fourier Transform Infrared Spectrometer (FTIR spectrometer) using KBr particles, the absorption spectrum in the range of 400-4000 cm^{-1} was recorded. The powder X-ray diffraction (XRD) pattern using Cu-Ka irradiation (λ=1.54056Å) was measured on a Bruker D8 Advance in the 2θ range of 20-80°. Scanning electron microscopy (SEM) images are characterized by Hitachi SU70 SEM coupling with an energy dispersive X-ray (EDX) detector. Transmission electron microscope (TEM) images were obtained from Tecnai G2 F20. X-ray photoelectron spectroscopy (XPS) analysis was performed on the AXIS ULTRA DLD electronic spectrometer by the Mg Ka (1253.6eV) achromatic X-ray source. Brunauer Emmett-Teller (BET) surface area was captured by N_2 adsorption measurement using Nova 2000E at 77.3 K. Brunauer Emmett-Teller (BET) surface area was captured by N_2 adsorption measurement using Nova 2000E at 77.3 K.

1.2 Electrode preparation and electrochemical characterization for SCs

Preparation of glassy carbon electrode(GCE): The composite electrode is made by mixing the active material and conductive carbon black with a mass ratio of 1:4. Weigh 5mg {$Cu_2SiW_{12}O_{40}$}@HKUST-1 and add certain naphthol as dispersant, disperse it ultrasonically for 40min to get a uniform turbid liquid. We used a pipette to remove 5μL drops on a pretreated glassy carbon electrode with a diameter of 3mm. After drying at room temperature, μL of 0.5% Nafion solution was dropped on the surface of the glassy carbon electrode, and dried in vacuum as the working electrode.

Preparation of nickel foam(NF) electrode: The NF was sonicated first with acetone for 30min and subsequently with 3 M HCl for 30 min. Thereafter, it was washed with distilled water and ethanol and then placed in a vacuum oven. Grind and mix the active material and acetylene black in a ratio of 1:1, add a certain amount of ethanol to dissolve ultrasonically, cut the nickel foam into 1×3cm^2 size, and apply 3mg to the nickel foam. Using a tablet press, the nickel foam was pressed into a sheet at 2MPa for 8 seconds.

Assembly of symmetrical button batteries: Cut two foam nickel sheets with a diameter of 1cm, apply the material to the foam nickel and press with a tablet machine. Put a piece into the positive electrode shell of the button electrode, then add a few drops of Na_2SO_4(1M) solution. Then add a diaphragm. Put another piece of nickel foam on top, then add one or two drops of Na_2SO_4 (1M). Put the metal plate shrapnel on it, and finally put the negative electrode.

Preparation of electrocatalytic water electrode: Grind the active material and acetylene black at a ratio of 2:1, weigh 5mg {$Cu_2SiW_{12}O_{40}$}@HKUST-1 and add ethanol as a dispersant to it, and ultrasonically form a uniform solution. We use a pipette to drop 5μL on the pretreated glassy carbon electrode with a diameter of 3mm. At room temperature, 7μL of 0.5% Nafion solution was dropped on the surface of the glassy carbon electrode and dried in a vacuum as a working electrode.

$$i = \mathrm{a}v^{\mathrm{b}} \qquad \text{Equation(S1)}$$

Where *i* is the peak current density, *v* is scan rate, and a and b are coefficients.

$$Q = Q_{\mathrm{C}} + Q_{\mathrm{d}} \qquad \text{Equation(S2)}$$

The surface treatment controls charge (Qc). the diffusion control charge (Qd)

$$Q = Q_C + kv^{-1/2}$$ Equation(S3)

Where k = variable parameter. Q = stored charge, v = scan rate.

$$C = \frac{2i_{\mathrm{m}} \int V dt}{V^2 \left| \frac{V_f}{V_i} \right.}$$ Equation(S4)

C(F g^{-1}) is the specific capacitance of the constant current charge and discharge curve. i_m(A g^{-1}) represents the current density, ∫Vdt is the current in the integration region, V_i and V_f represent the initial and final values of the potential.

$$Cs = I \cdot t / (m \cdot \Delta V)$$ Equation(S5)

Where C_s represents the specific capacitance, *I* is the charge and discharge current(A), t is the discharge time(s), m(g) represents thIe load mass of the active material, and ΔV is the voltage difference (V).

2. Results and Discussion

2.1 The characterization diagrams

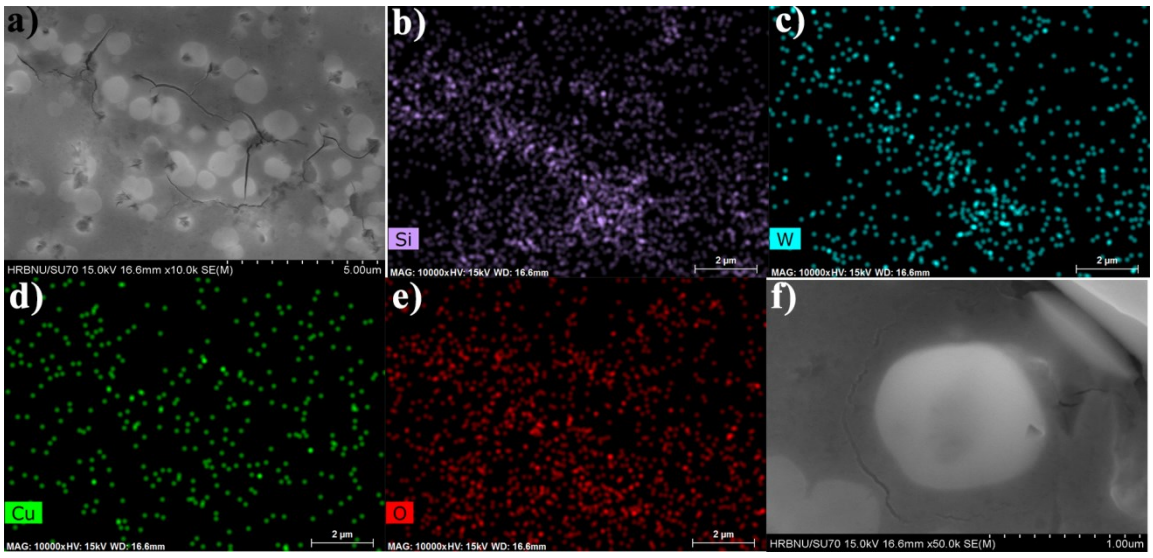

Figure S1 (a,f) SEM images; (b-e) EDX of Si, W, Cu and O of $Cu_2SiW_{12}O_{40}$.

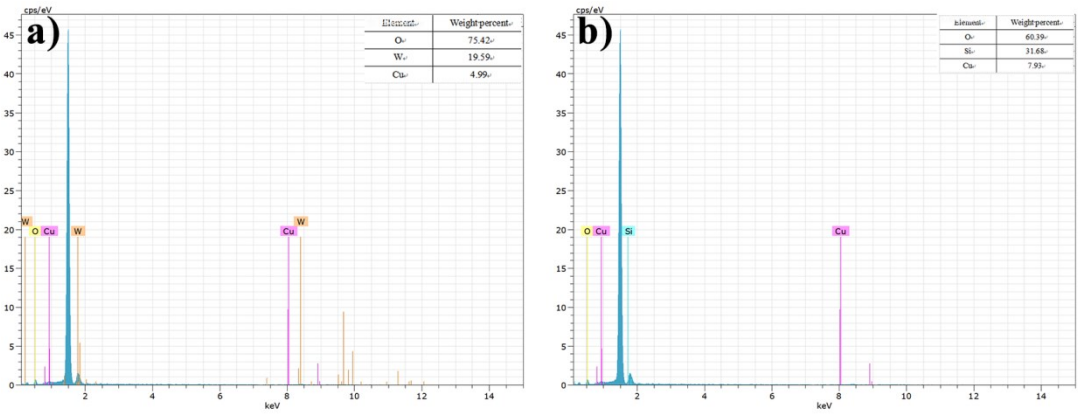

Figure S2. EDS of $Cu_2SiW_{12}O_{40}$.

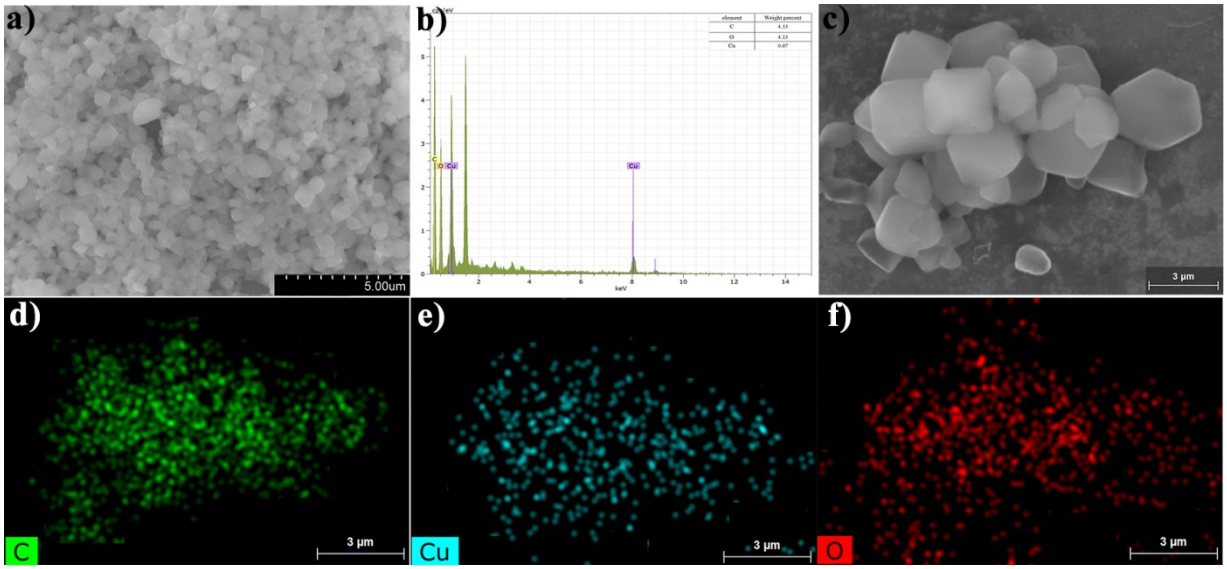

Figure S3. (a,c) SEM images; (b) EDS of HKUST-1. (d-f) EDX of C, Cu and O of HKUST-1.

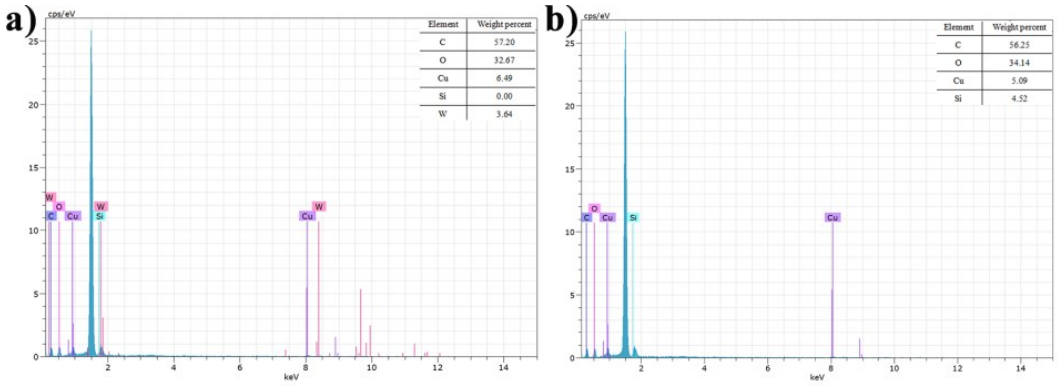

Figure S4. EDS of $\{Cu_2SiW_{12}O_{40}\}$@HKUST-1.

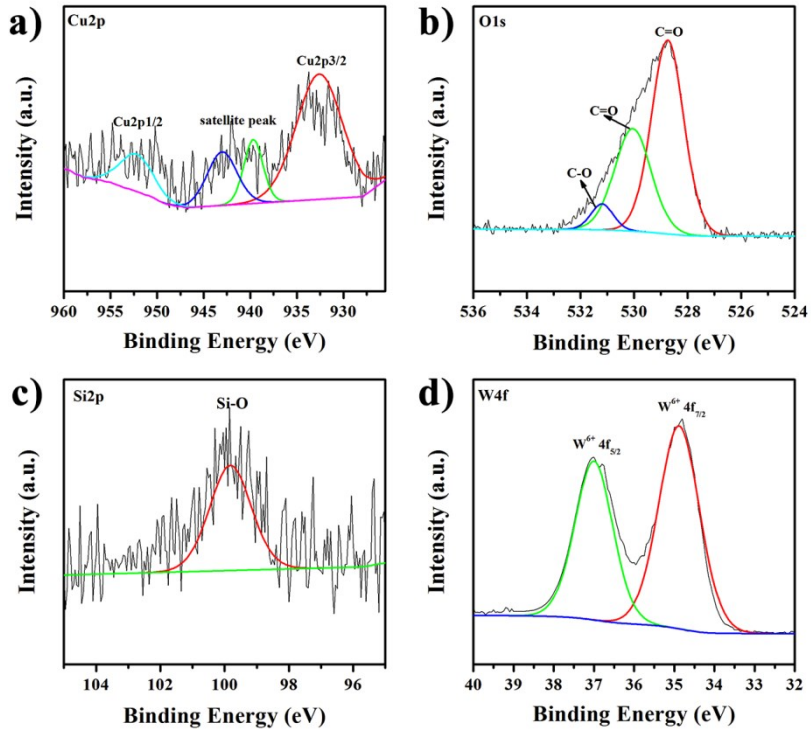

Figure S5. XPS spectra of $Cu_2SiW_{12}O_{40:}$ (a) Cu, (b) O, (c) Si and (d) W.

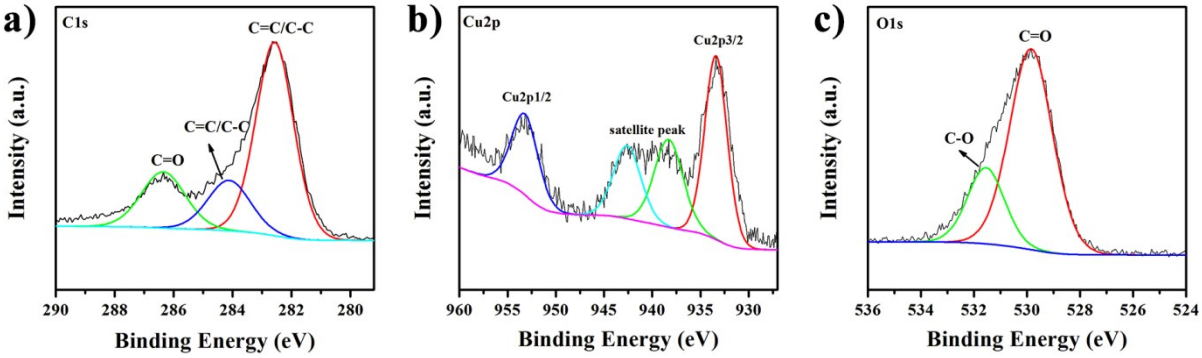

Figure S6. XPS spectra of HKUST-1: (a) C, (b) Cu and (c) O.

2.2 Supercapacitor test chart of compounds

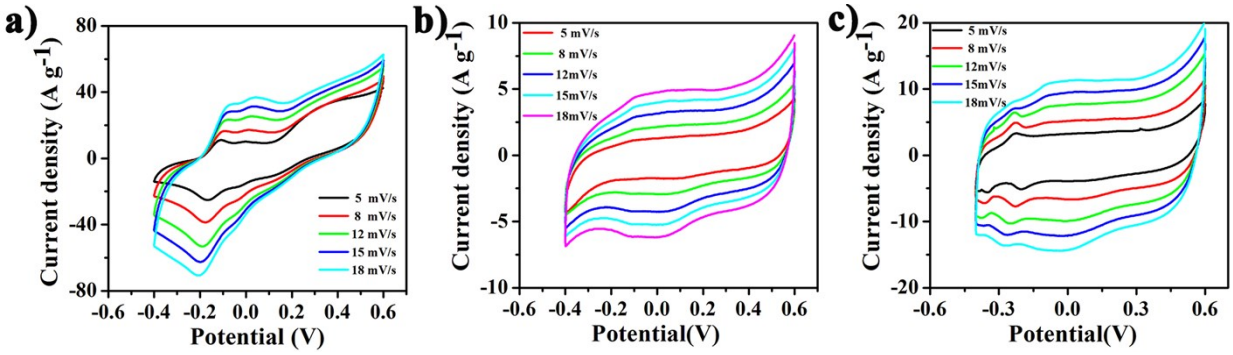

Figure S7. The CVs at different scan rates:(a) $\{Cu_2SiW_{12}O_{40}\}$@HKUST-1, (b) $Cu_2SiW_{12}O_{40}$. (c)HKUST-1.

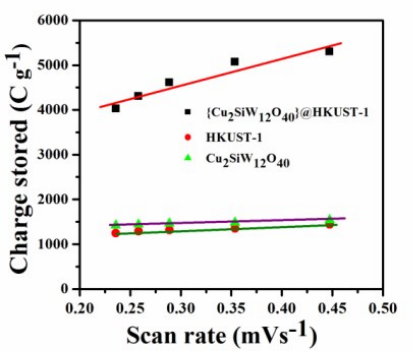

Figure S8. Plot of the total charge stored (q) vs. the reciprocal of the square root of the scan rate.

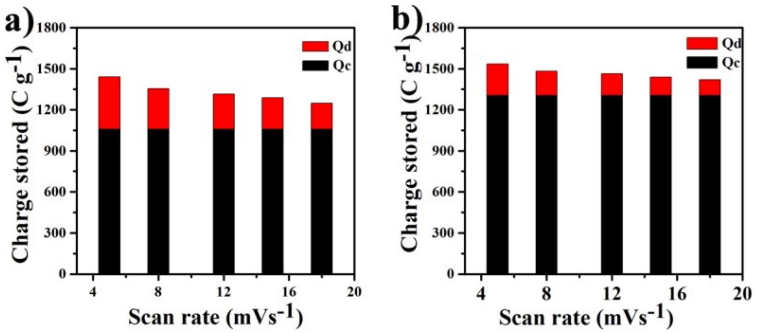

Figure S9. Normalized contribution ratio of the capacitive (Q_c) and diffusion-controlled (Q_d) charge storage capacities at lower scan rates of (a) HKUST-1, (b) $Cu_2SiW_{12}O_{40}$.

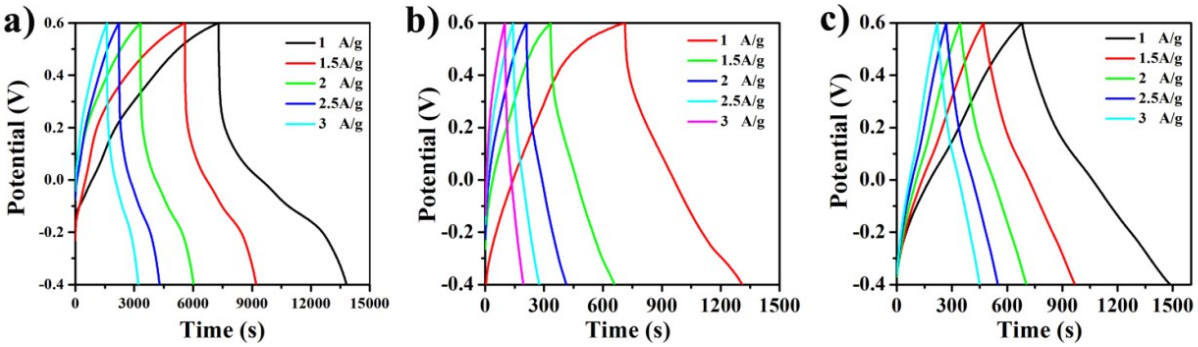

Figure S10. The GCD of (a){$Cu_2SiW_{12}O_{40}$}@HKUST-1, (b)HKUST-1,(c)$Cu_2SiW_{12}O_{40}$ at different current densities.

2.3 Electrocatalytic water oxygen production diagram of compounds

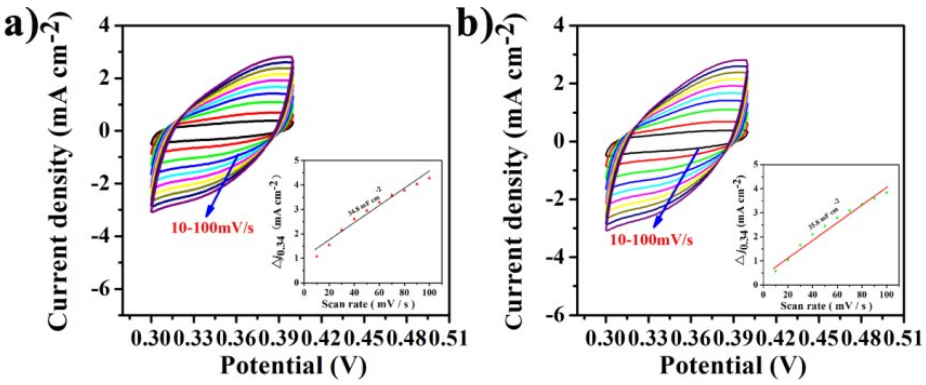

Figure S11. CVs of (a) HKUST-1; (b) $Cu_2SiW_{12}O_{40}$ with different rates from 10 to 100 mV s^{-1}. Inset: The capacitive current at 0.34V as a function of the scan rate for (a) HKUST-1. (b) $Cu_2SiW_{12}O_{40}$.

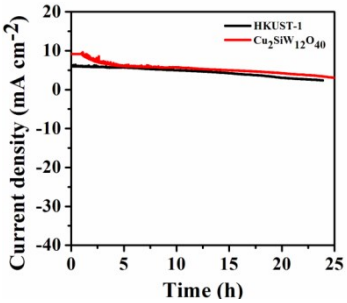

Figure S12. Time-dependent current density curve of HKUST-1 and $Cu_2SiW_{12}O_{40}$.

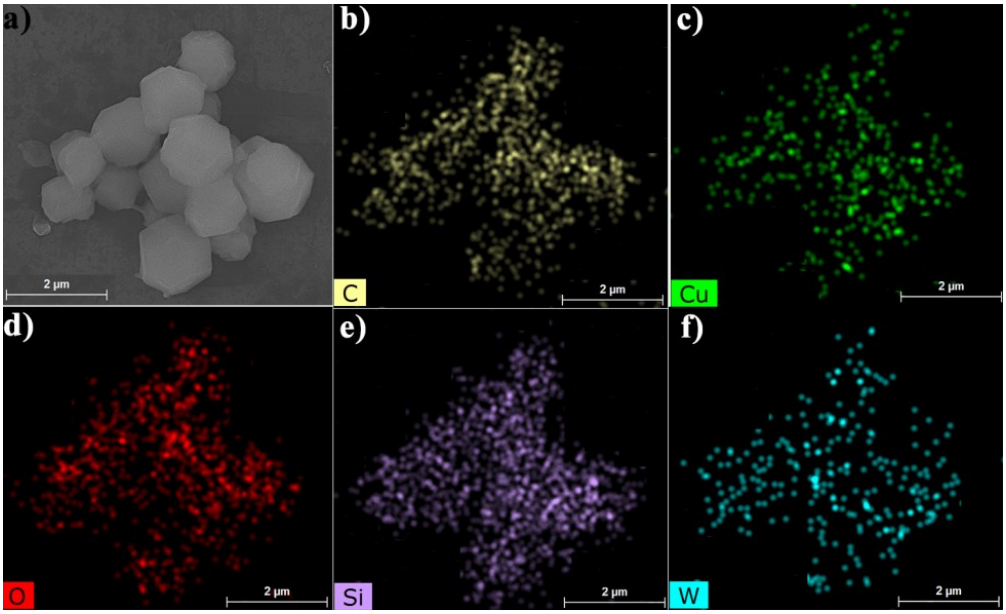

Figure S13. (a)SEM image of the {$Cu_2SiW_{12}O_{40}$}@HKUST-1 catalyst after OER stability test, (b-f) EDX of C, Cu, O, Si and W.

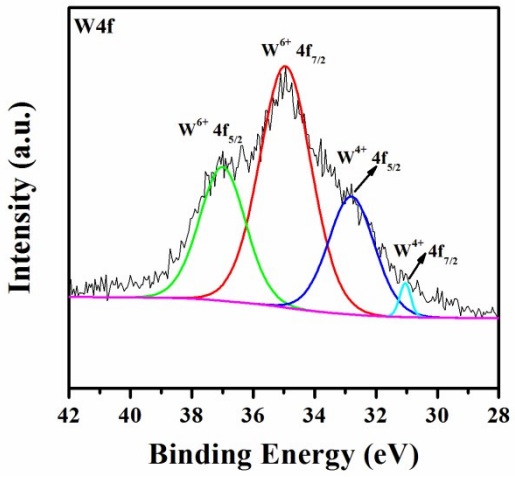

Figure S14. The W4f XPS spectra of {$Cu_2SiW_{12}O_{40}$}@HKUST-1 after OER tests.

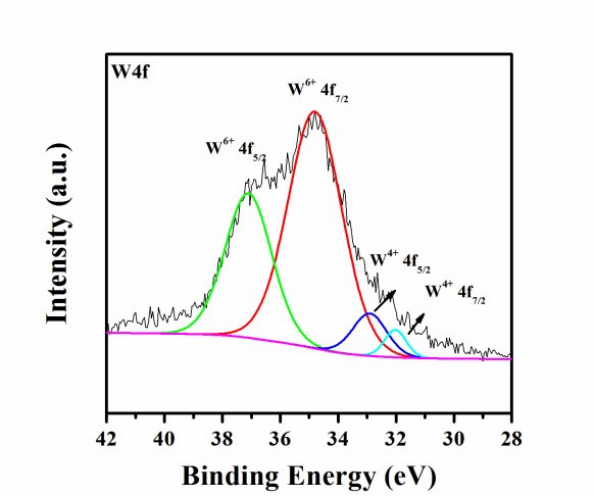

Figure S15. The W4f XPS spectra of $Cu_2SiW_{12}O_{40}$ after OER tests.

2.4 Comparison of the properties of the Keggin-based materials with published supercapacitors

Table S1 Comparison of the properties of the Keggin-based materials with published supercapacitors

	Compound	The capacitances	The cyclic stability	collector	Ref
1	PAni/$H_3PMo_{12}O_{40}$	120F g^{-1}	70% (1000 cycles)	Rigid graphite plate	[1]
2	MWCNT/$Cs_xPMo_{12}O_{40}$	285 F g^{-1} (0.2 A g^{-1})	----		[2]
3	$H_3PMo_{12}O_{40}$/MWCNT	38 F g^{-1} (1 A g^{-1})	----------	porous glassy fibrous paper	[3]
4	$[BMIM]_4SiW_{12}O_{40}$	172 F g^{-1} (20 mV s^{-1})	89% (1100 cycles)	glassy carbon	[4]
5	AC/$PMo_{12}O_{40}$	140 F g^{-1} (1 A g^{-1})	91% (8000 cycles)	glassy carbon	[5]
6	AC/$PW_{12}O_{40}$	254 F g^{-1} (10 mV s^{-1})	35% (30000 cycles)	Graphite rods	[6]
7	RGO/PIL/ $PMo_{12}O_{40}$	408 F g^{-1}	98% (2000 cycles)	stainless steel foil	[7]
8	rGO/$PMo_{12}O_{40}$	276 F g^{-1}	96% (10000 cycles)	Graphite roods	[8]

9	SWCNT/TBA/$PMo_{12}V_2O_{40}$	444 F g^{-1} (10 mV s^{-1})	95% (6500 cycles)	glassy carbon rods and graphite papers	[9]
10	rGO/ $PMo_{12}O_{40}$	51.2 F g^{-1}	95% (5000 cycles)	commercial flexible carbon cloth	[10]
11	AC/$PMo_{12}O_{40}$	223F g^{-1}	100% (10000 cycles)	Ti foils	[11]
12	PMo_{12}–$XWxO_{40}^{3-}$	140 F g^{-1} (10 A g^{-1})	94.6% (1700cycles)	glassy carbon	[12]
13	$[Ag_5(brtmb)_4][VW_{10}V_2O_{40}]$	206 F g^{-1} (110 A g^{-1})	81.7% (1000 cycles)	glassy carbon	[13]
14	Pinecone AC/$PMo_{12}O_{40}$	361 F g^{-1}	-----	titanium foil	[14]
15	AC/$PMo_{12}O_{40}$	293F g^{-1}	-----	C250 carbon monoliths	[15]
16	$[Ag_5(brtmb)_4][VW_{10}V_2O_{40}]$	206 F g^{-1} (110 A g–1)	81.7% (1000 cycles)	glassy carbon	[16]
17	rGO-PMo_{12}	278 mF cm^{-2}	89% (5000 cycles)	Carbon cloth	[17]
18	rGO-PMo_{12}‖rGO-PW_{12}	110 F cm^{-2} (2 mA cm^{-2})	95% (2000 cycles)	carbon cloth	[17]
19	$[Cu^{I}(btx)]_4[SiW_{12}O_{40}]$	110.3 F g^{-1} (3.0 A g^{-1})	87% (1000 cycles)	glassy carbon	[18]
20	NENU-5/PPy	779.8 F g^{-1} (10 mV s^{-1})	-----	carbon cloth	[19]
21	$[H(C_{10}H_{10}N_2)Cu_2][PMo_{12}O_{40}]$	287 F g^{-1} (1 A g^{-1})	81.5% (500 cycles)	glassy carbon	[20]
22	$[H(C_{10}H_{10}N_2)Cu_2][PW_{12}O_{40}]$	153.43F g^{-1} (1A g^{-1})	18.2% (500 cycles)	glassy carbon	[20]
23	$NiPW_{12}$NP/FrGO	437.6 F g^{-1} (4 A g^{-1})	94.3% (5000 cycles)	carbon paper	[21]
24	mPPy@GO-PMo_{12}	115 mF cm^{-2} (1 mV s^{-1})	80% (2000 cycles)	glassy carbon	[22]
25	$[Ag_5(C_2H_2N_3)_6][H_5\square SiMo_{12}O_{40}]$@15%GO	230.2 F g^{-1} (0.5 A g^{-1})	92.7% (1000 cycles)	glassy carbon	[23]
26	$[Cu^{I}H_2(C_{12}H_{12}N_6)(PMo_{12}O_{40})]\cdot[(C_6H_{15}N)(H_2O)_2]$	249 F g^{-1} (3 A g^{-1})	93.5% (1000 cycles)	glassy carbon	[24]
27	$[Cu^{II}_2(C_{12}H_{12}N_6)_4(PMo^{VI}_9Mo^{V}_3O_{39})]$	154.5F g^{-1} (3A g^{-1})	91.1% (1000 cycles)	glassy carbon	[24]

28	$[Cu^{I}_4H_2(btx)_5(PMo_{12}O_{40})_2]\cdot 2H_2O$	237 F g^{-1} (2 A g^{-1})	92.5% (1000 cycles)	glassy carbon	[25]
29	$[Cu^{I}_4H_2(btx)_5(PW_{12}O_{40})_2]\cdot 2H_2O$	100F g^{-1} (2A g^{-1})	90% (1000cycles)	glassy carbon	[25]
30	$[Cu^{II}Cu^{I}_3(H_2O)_2(btx)_5(PW^{VI}_{10}W^{V}_2O_{40})]\cdot 2H_2O$	82.1F g^{-1} (2A g^{-1})	100% (1000cycles)	glassy carbon	[25]
31	$[Cu^{I}_6(btx)_6(PW^{VI}_9W^{V}_3O_{40})]\cdot 2H_2O$	76.4F g^{-1} (2A g^{-1})	100% (1000cycles)	glassy carbon	[25]
32	$[Cu^{II}Cu^{I}_3(btx)_5(SiMo^{VI}_{11}Mo^{V}O_{40})]\cdot 4H_2O$	138.4F g^{-1} (2A g^{-1})	97% (1000cycles)	glassy carbon	[25]
33	$[\{Ag_5(pz)_7\}(BW_{12}O_{40})]$	1058 F g^{-1} (2.16 A g^{-1})	90.3% (1000 cycles)	glassy carbon	[26]
34	$[\{Ag_5(pz)_7\}(SiW_{12}O_{40})](OH)\cdot H_2O$	986F g^{-1} (2.16A g^{-1})	94.5% (1000 cycles)	glassy carbon	[26]
35	$(Hpyr)[\{Ag(pz)\}_2(PMo_{12}O_{40})$	1611F g^{-1} (2.16A g^{-1})	84.8% (1000 cycles)	glassy carbon	[26]
36	$[Cu^{I}_3(pz)_2(phen)_3]_2\,[Cu^{I}(phen)_2]\,[\{Na(H_2O)_2\}\{(V^{IV}_5Cu^{II}O_6)(As^{III}W_9O_{33})_2\}]\cdot 6H_2O$	825 F g^{-1} (2.4 A g^{-1})	91.4% (3000 cycles)	glassy carbon	[27]
37	$[Ag_5(C_2H_2N_3)_6][H_5SiMo_{12}O_{40}]$@15%GO-based electrode	230.2F g^{-1} (0.5A g^{-1})	92.7% (1000cycles)	glassy carbon	[28]
38	$[Ag(bpy)][\{Ag(Hbpy)\}_2(AlW_{12}O_{40})]\cdot H_2O$	478.41 F g^{-1} (1 A g^{-1})	95.71% (5000 cycles)	carbon cloth	[29]
39	$[H_2en][\{Cu(bpy)\}_3(AlW_{12}O_{40})]\cdot 3H_2O$	625.99 F g^{-1} (1 A g^{-1})	97.62% (5000 cycles)	carbon cloth	[29]
40	$[Ni(itmb)_4(HPMo_{12}O_{40})]\cdot 2H_2O$	477.9 F g^{-1} (15 A g^{-1})	------	glassy carbon	[30]
41	$[Zn(itmb)_3(H_2O)(HPMo_{12}O_{40})]\cdot 4H_2O$	890.2 F g^{-1} (15 A g^{-1})	------	glassy carbon	[30]
42	$[Mn_2(BTC)_{4/3}(H_2O)_6]_6\,[K_8(SiW_{10}Mn_2Cl_4O_{36})]$	211.0 F g^{-1} (1 A g^{-1})	96.0% (5000 cycles)	nickel foam	[31]
43	PPD-PMo_{12}@rGO	790 F g^{-1} (1 mV s^{-1})	90.5% (30 000 cycles)	carbon paper	[32]
44	PPD-PMo_{12}	550 F g^{-1} (1 mV s^{-1})		Carbon paper	[32]
45	PMo_{12}@GO	305 F g^{-1} (1 mV s^{-1})		carbon paper	[32]
46	$(imi)_2[\{Ag_3(tpb)_2\}_2(H_2O)\{AsW_{12}O_{40}\}_2]\cdot 6H_2O$	929.7 F g^{-1} (3.6 A g^{-1})	89.6% (5000 cycles)	glassy carbon	[33]
47	$[(Ag_7bpy_7Cl_2)\{AsW^{V}_2W^{VI}_{10}O_{40}\}]\cdot H_2O$	986.1 F g^{-1} (3.6 A g^{-1})	91.4% (5000 cycles)	glassy carbon	[33]

48	AC/TEAPW$_{12}$	82 F g^{-1} (0.5 A g^{-1})	93% (10000 cycles)	aluminum foil	[34]
49	[HPMo$_{12}$O$_{40}$]@[Cu$_4$(μ_2-OH)$_2$(C$_6$H$_5$PO$_3$)$_2$(bimb)$_4$]	267.0F g^{-1} (5 A g^{-1})	95.1% (1000 cycles)	glassy carbon	[35]
50	PMo$_{10}$V$_2$@ZIF-67	475 F g-1 (2 A g^{-1})	106.41% (5000 cycles)	Ni foam	[36]
51	{Cu$_2$SiW$_{12}$O$_{40}$}@HKUST-1	5096.5F g^{-1} (1 A g^{-1})	92% (6000 cycles)	glassy carbon	This work
52	H$_4$SiW$_{12}$O$_{40}$	604.6F g^{-1} (1 A g^{-1})	82% (6000 cycles)	glassy carbon	This work
53	{Cu$_2$SiW$_{12}$O$_{40}$}@HKUST-1	403.7F g^{-1}(1 A g^{-1})	91.7% (6000 cycles)	nickel foam	This work

References

[1] A. K. C. Gallegos, M. L. Cantú, N. C. Pastor, P. G. Romero, *Adv. Funct. Mater.,* 2005, **15**, 1125-1133. DOI:org/10.1002/adfm.200400326

[2] A. K. C. Gallegos, R. M. Rosales, M. Baibarac, P. G. Romero, M. E. Rincón, *Electrochem. Commun.,* 2007, **9**, 2088-2092. DOI:10.1016/ j.elecom.2007.06.003

[3] M. Skunik, M. Chojak, I. A. Rutkowska, P. J. Kulesza, *Electrochim. Acta*, 2008, **53**, 3862-3869. DOI:10.1016/j.electacta.2007.11.049

[4] M. Ammam, J. Fransaer, *J. Electron. Mater.*, 2011, **158**, A14-A21. DOI:org/10.1149/1.3507254

[5] V. Ruiz, J. S. Guevara, P. G. Romero, *Electrochem. Commun*., 2012, **24**, 35-38. DOI:10.1016/j.elecom.2012.08.003

[6] J. S. Guevar,V. Ruiz, P. G. Romero, *J. Mater. Chem. A,* 2014, **2**, 1014-1021. DOI:10.1039/c3ta14455k

[7] M. H. Yang, B. G. Choi, S. C. Jung, Y. K. Han, Y. S. Huh, S. B. Lee, *Adv. Funct. Mater.* 2014, **24**, 7301-7309. DOI:10.1002/adfm.201401798

[8] J. S. Guevara, V. Ruiza, P. G. Romero, *Phys. Chem. Chem. Phys.,* 2014, **16**, 20411-20414. DOI:10.1039/C4CP03321C

[9] H. Y. Chen, R. A. Oweini, J. Friedl, C. Y. Lee, L. L. Li, U. Kortz, U. Stimming, M. Srinivasan, *Nanoscale,* 2015, **7**, 7934-7941. DOI:10.1039/c4nr07528e

[10] D. P. Dubal, J. S.Guevara, D. Tonti, E. Encisoc, P. G. Romero, *J. Mater. Chem. A,* 2015, **3**, 23483-23492. DOI: 10.1039/C5TA05660H

[11] C. C. Hu, E. B. Zhao, N. Nitta, Magasinski, G. Berdichevsky, G.Yushin, *J. Power Source*s, 2016, **326**, 569-574. DOI:10.1016/j.jpowsour.2016.04.036

[12] Y. H. Ding, J. Peng, H. Y. Lu, Y. Yuan, *RSC Adv.*, 2016, **6**, 81085-81091, DOI: 10.1039/C6RA15381J.

[13] G. N. Wang, T. T. Chen, X. M. Wang, H. Y. Ma, H. J. Pang, *Eur. J. inorg. Chem.*, 2017, **2017,** 5350-5355. DOI: 10.1002/ejic.201701031

[14] M. Genovese and K. Lian, *J. Mater. Chem. A*, 2017, **5**, 3939-3947. DOI: 10.1039/C6TA10382K

[15] P. Palomino, J. S. Guevara,M. O. Marínc, V. Ruiz, D. P. Dubal, P. G.Romero, D.Tonti, E.Enciso, *Carbon*, 2017, **111**, 74-82. DOI: 10.1016/j.carbon.2016.09.054

[16] G. N. Wang, T. T. Chen, X. M. Wang, H. Y. Ma, H. J. Pang, Eur. J. Inorg. Chem., 2017, **45**, 5350-5355. DOI:10.1002/ejic.201701031

[17] D. P. Dubal, N. R. Chodankar, A. Vinu, D. H. Kim, P. Gomez-Romero, *ChemSusChem,* 2017, **10**, 2742-2750. DOI: 10.1002/cssc.201700792

[18] D. F. Chai, Y. Hou, K. P. O'Halloran, H. J. Pang, H. Y. Ma, G. N. Wang, X. M. Wang, *Chem. Electro. Chem*., 2018, **5**, 3443-3450. DOI: 10.1002/celc.201801081

[19] H. N. Wang, M. Zhang, A. M. Zhang, F. C. Shen, X. K. Wang, S. N. Sun, Y. J. Chen, Y. Q. Lan, *ACS Appl. Mater. Interfaces,* 2018, **10**, 32265-32270. DOI: 10.1021/acsami.8b12194

[20] S. Roy, V. Vemuri, S. Maiti, K. S. Manoj, U. Subbarao, and S. C. Peter, *Inorg. Chem.,* 2018, **57**, 12078-12092. DOI: 10.1021/acs.inorgchem.8b01631

[21] X. G. Sang, X. X. Xu, L. J. Bian, X. X. Liu, Y. Wang, *Solid State Sci.,* 2018, **83**, 8-16, DOI:10.1016/j.solidstatesciences.2018.06.006.

[22] J. Q. Qin, F. Zhou, H. Xiao, R. Y. Ren, Z. S. Wu, *Sci. China Mater.*, 2018, **61**, 233-242. DOI:10.1007/s40843-017-9132-8.

[23] Y. Hou, D. F. Chai,B. N. Li, H. J. Pang, H. Y. Ma, X. M. Wang, L. C. Tan, *ACS Appl. Mater. Interfaces*, 2019, **11**, 20845-20853. DOI: 10.1021/acsami.9b04649

[24] D. F. Chai, J. J. Xin, B. N. Li, H.J. Pang, H. Y. Ma, K. Q. Li, B. X. Xiao, X. M. Wanga and L. C. Tana, *Dalton Trans.*, 2019, **48**, 13026-13033. DOI:10.1039/C9DT02420D

[25] D. F. Chai, Carlos J. Gómez-García, B. N. Li, H. J. Pang, H. Y. Ma, X. M. Wang, L. C. Tan, Chem. Eng. J., 2019, **373**, 587-597. DOI:10.1016/j.cej.2019.05.084

[26] N. N. Du, L. G. Gong, L. Y. Fan, K. Yu, H. Luo, S. J. Pang, J. Q. Gao, Z. W. Zheng, J. H. Lv,and B. B. Zhou, *ACS Appl. Nano Mater.,* 2019, **2**, 3039-3049. DOI: 10.1021/acsanm.9b00409

[27] K. P. Wang, K. Yu, J. H. Lv, M. L. Zhang, F. X. Meng, and B. B. Zhou, *Inorg. Chem.,* 2019, **58**, 7947-7957. DOI: 10.1021/acs.inorgchem.9b00692

[28] Y. Hou, D. F. Chai, B. N. Li, H. J. Pang, H. Y. Ma, X. M. Wang, L. C. Tan, *ACS Appl. Mater. Interfaces,* 2019, **11**, 20845-20853.DOI:10.1021/acsami.9b04649

[29] L. G. Gong, X. X. Qi, K. Yu, J. Q. Gao, B. B. Zhou, G. Y. Yang. *J. Mater. Chem. A,* 2020, **8**, 5709-5720. DOI:10.1039/C9ta14103k

[30] G. N. Wang, T. T. Chen, C. J. G. García, F. Zhang, M. Y. Zhang, H. Y. Ma, H. J. Pang, X. M. Wang, L. C. Tan, *Small,* 2020, **16**, 2001626, DOI: 10.1002/smll.202001626

[31] Z. W. Zheng, X. Y. Zhao, L. G. Gong, C. X. Wang, C. M. Wang, K. Yu, B. B. Zhou, *J. Solid State Chem.*, 2020, **288**, 121409, DOI: 10.1016 /j.jssc.2020.121409

[32] J. Gao, M. X. Tong, Z. Y. Xing, Q. Y. Jin, J. X. Zhou, L. L. Chen, H. L. Xu, G. H. Li, *Chem. Commun.*, 2020, **56**, 7305-7308. DOI: 10.1039/d0cc02464c

[33] L. P. Cui, K. Yu, J. H. Lv, C. H. Guo, B. B. Zhou, *J. Mater. Chem. A,* 2020, **8**, 22918-22928, DOI:10.1039/D0TA08759A

[34] J. J. Zhu, R. B. Vilaua, P. G. Romero, *Electrochim. Acta*, 2020, **362**, 137007, DOI:10.1016/j.electacta.2020.137007

[35] S. B. Li, X. G. Tan, M. Yue, L. Zhang, D. F. Chai, W. D. Wang, H. Pan, L.L. Fan, *Chem. Commun.,* 2020, **56**, 15177-15180. DOI:10.1039/D0CC06665F

[36] A. M. Mohamed, M. Ramadan, N. Ahmed, A. O. A. ElNaga, H. H. Alalawy, T. Zaki, S. A. Shaban, H. B. Hassan, N. K. Allam, *J. Energy Storage*, 2020, **28**, 101292, DOI:10.1016/j.est.2020.101292